Journal of Applied Polymer Science

Preparation of AgCl/polyaniline nanocomposite in polyvinylalcohol matrix and its electrocatalytic activity

Soghra Fathalipour, Bakhshali Massoumi
Department of Chemistry, Payame Noor University, Tehran, Iran
Correspondence to: S. Fathalipour (E-mail: fathalipour@pnu.ac.ir)

ABSTRACT: AgCl/polyaniline (PANI) nanocomposite was successfully synthesized in polyvinyl alcohol (PVA) matrix via a two-stage process. Firstly, positively-charged Ag nanoparticles (NPs) were prepared in the presence of 4-aminothiophenole (4-ATP) as stabilizer. Then, polymerization of aniline was carried out in PVA matrix in the presence of Ag NPs, HCl, and ammonium persulfate as oxidant. HCl solution played an important role in the preparation of resulted nanocomposite. Removal or changing of acidic medium to camphorsulfonic acid influenced on the structure and morphology of obtained composites. The composites were characterized by scanning electron microscopy, transmission electron microscopy, X-ray diffraction, energy-dispersive X-ray spectroscopy, ultraviolet–visible spectra, and Fourier transform infrared spectroscopy. Moreover, AgCl/PANI/PVA nanocomposite was immobilized on the surface of a glassy carbon electrode and showed enhanced electrocatalytic activity for the oxidation of dopamine (DA) in a neutral solution. The peak currents of differential pulse voltammograms of DA increased linearly with concentration in the ranges of 80–250 μM DA and the detection limit for DA was 17.2 μM. © 2015 Wiley Periodicals, Inc. J. Appl. Polym. Sci. **2015**, *132*, 42366.

KEYWORDS: colloids; composites; electrochemistry

Received 25 November 2014; accepted 12 April 2015
DOI: 10.1002/app.42366

INTRODUCTION

Polyaniline (PANI) is known among conducting polymers due to its high conductivity, ease of preparation, good environmental stability, and a large variety of technological applications in rechargeable batteries, chemical sensors, electromagnetic interference shielding (EMI), corrosion protection coatings, light emitting diodes, and etc.[1–4] However, PANI is redox-active only for acidic conditions, generally at pH < 4;[1,2] this seriously has obstructed its potential applications in bioelectrochemistry, which normally needs a neutral pH environment. In order to overcome such problems, several approaches have been developed. For instance, the incorporation of inorganic nanoparticles (NPs) could effectively improve the electrical, optical and dielectric properties of the PANI composites.[5,6]

The inorganic nanocomposites with different combinations have concerned significant academic and technological attention because they have interesting physical properties and potential applications.[7,8] The ability to control the shape and size of nanocomposites is a chief factor for defining of their properties, such as the electronic band gap, conductivity, and light-emission efficiency.[9,10] Among those inorganic nanoparticles, silver nanoparticles (NPs) and silver (Ag) nanograin decorated AgCl NPs, and aggregated Ag nanoparticles have received a great deal of attention because of their unique electrical and optical properties as well as extensive applications in preparation of photographic paper, photochromic lenses, photocatalyst, antiseptic catheters, bone cements, and fabrics owing to their antibacterial property.[11–13] It has been displayed that decoration of AgCl with Ag NPs can greatly recover the light absorption property and photostability of the AgCl nanoparticles.[14,15] Incorporation of Ag and AgCl NPs between the PANI chains could yield functional materials having unique properties and wide varieties of potential applications in various areas including electronic, catalysis, optics, electrocatalysis, and sensors. Hence, the synthesis of polyaniline/Ag and AgCl nanocomposites is receiving wide attention. Massoumi *et al.*[16] synthesized PANI–silver nanocomposites through *in situ* chemical polymerization of aniline in the presence of Ag NPs and reported its electrocatalytic activity toward the oxidation of dopamine (DA) and tyrosine (Ty) at pH:4. Choudhury[17] synthesized PANI–silver nanocomposites by *in situ* chemical oxidation polymerization method and reported superior gas sensing capacity of obtained nanocomposites compared to pure polyaniline. Zhang *et al.* synthesized polyaniline/AgCl nanocomposites at the water/magnetic ionic liquid interface.[18] Feng *et al.* prepared AgCl/PANI core–shell composites through a facile one-step process and used to construct a H_2O_2 biosensor.[19] Zhou *et al.* synthesized PANI/AgCl composites by electrochemical methods in the presence of polyvinyl pyrrolidone which exhibited strong

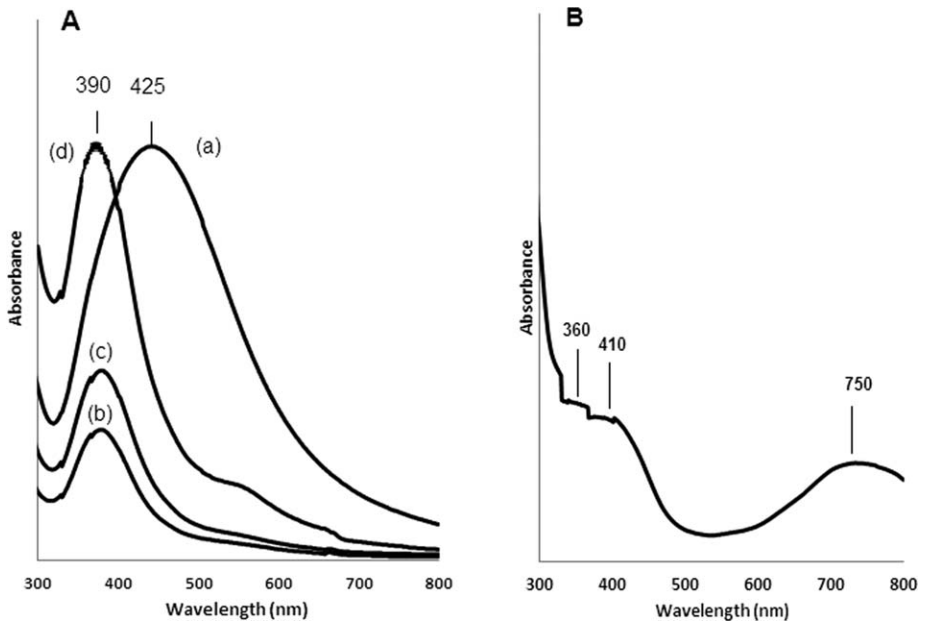

Figure 1. UV–vis spectrum of A: (a) Ag NPs colloid (b) AgCl/PANI/PVA (composite 1) (c) Ag/PANI/PVA (composite 4) (d) Ag oxides/CSA/PANI/PVA (composite 3). B: Filtrate of composite 1. All samples dispersed in ethanol absolute.

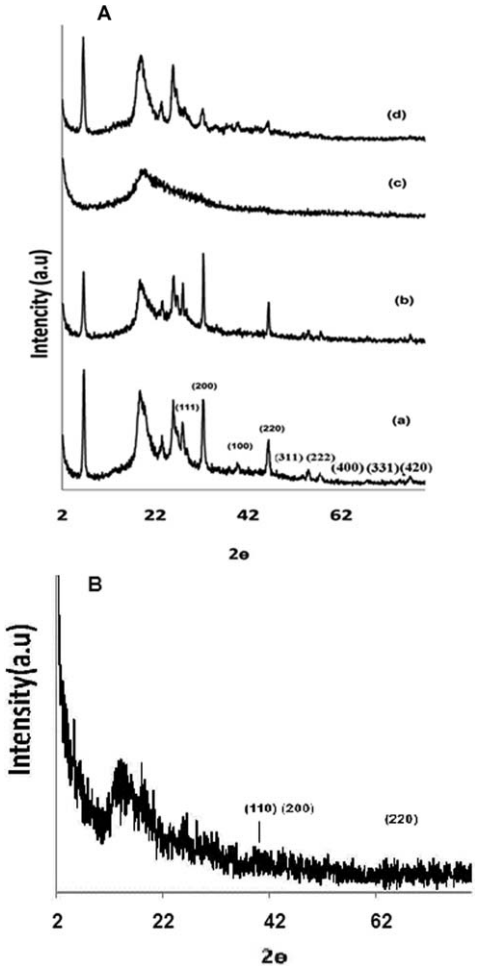

Figure 2. XRD pattern of A: (a) Ag/AgCl/PANI/PVA (composite 2) (b) AgCl/PANI/PVA (composite 1) (c) Filtrate of composite 1 (d) Ag oxides/CSA/PANI/PVA (composite 3) B: Ag/PANI/PVA (composite 4).

electrocatalytic activity toward the oxidation of DA and ascorbic acid (AA).[20] To application of PANI composites in the living system for continuous monitoring of the level of main metabolites such as sugar, cholesterol etc., it is essential that the sensor electrode to be biocompatible.

Polyvinyl alcohol (PVA), a water soluble hydrophilic polymer, is widely used in industries owing to its excellent chemical and physical properties, nontoxicity, excellent chemical resistance, good film formation capacity, biocompatibility and high crystal modulus. On the other hand the existence of PVA in the preparation of PANI composite increases crystallinity and stability in PANI and also decreases the size of PANI dispersion NPs.[21] To the best of knowledge, studies on the synthesizing of AgCl/PANI nanocomposite in PVA matrix through chemical polymerization are relatively rare. In this study, AgCl/PANI nanocomposite was prepared via *in situ* polymerization of aniline in the presence of Ag NPs in PVA matrix. The synthesis of nanocomposite was studied in different acidic medias and the morphology, optical properties and composition of the obtained composites were characterized by scanning electron microscopy (SEM), transmission electron microscopy (TEM), energy-dispersive X-ray spectroscopy (EDX), ultraviolet–visible spectroscopy (UV–vis), X-ray diffraction (XRD), and Fourier transform infrared spectroscopy (FT-IR). The obtained AgCl/PANI/PVA nanocomposite was immobilized on the surface of a glassy carbon electrode and investigated electrocatalytic activity for the oxidation of dopamine in a neutral solution.

EXPERIMENTAL

Materials and Methods

Aniline, ammonium persulfate ($(NH_4)_2S_2O_8$, APS), 4-aminothiophenol (4-ATP), hydrochloric acid (HCl), camphorsulfonic acid (CSA), sodium borohydride ($NaBH_4$), silver nitrate

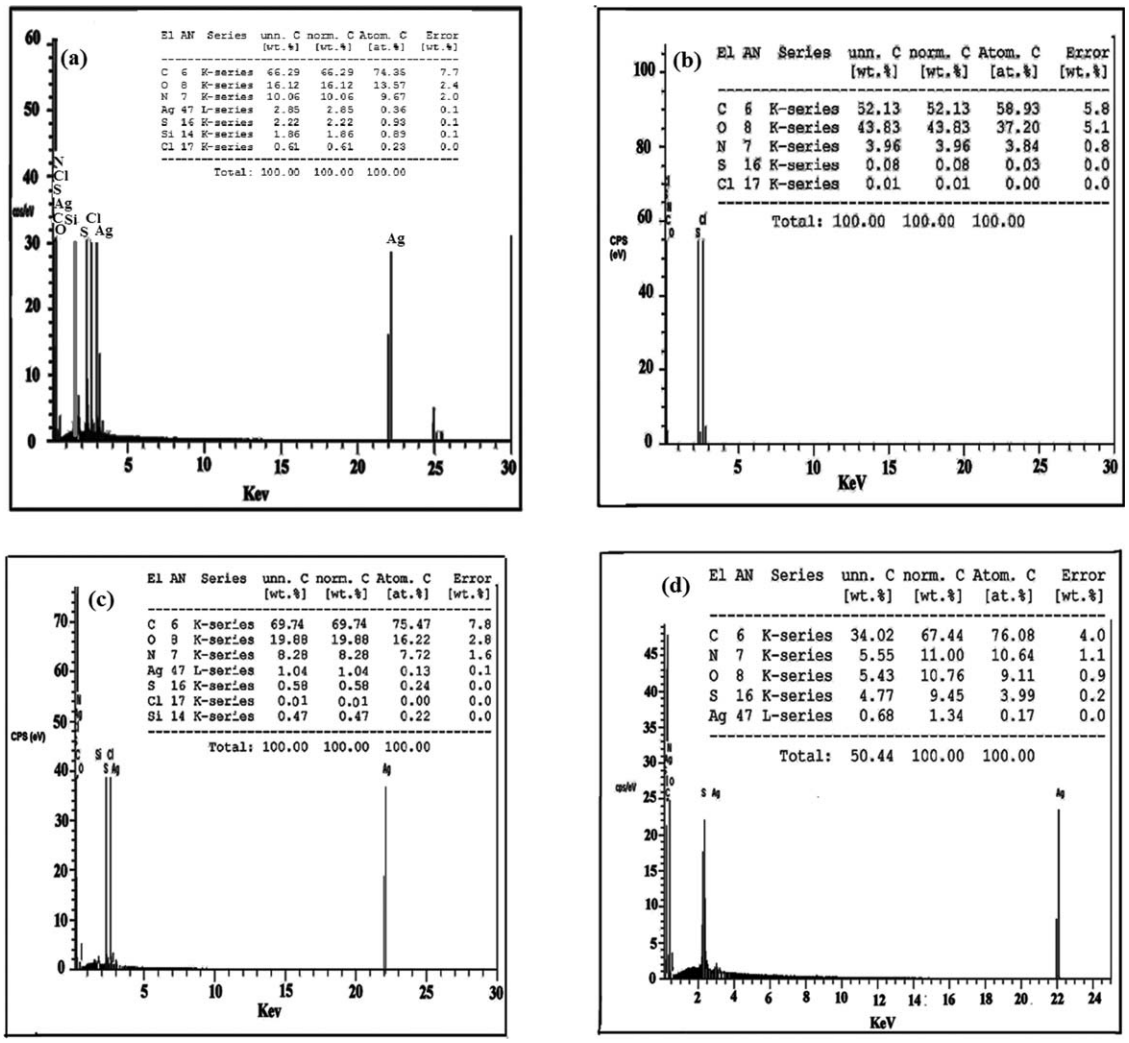

Figure 3. EDX analysis of (a) AgCl/PANI/PVA (composite 1) (b) filtrate of composites 1 (c) Ag oxides/CSA/PANI/PVA (composite 3) (d) Ag/PANI/PVA (composite 4).

($AgNO_3$), polyvinyl alcohol (PVA, 98% hydrolyzed, molecular weight of 72,000 g/mol), and dopamine (DA) were purchased from Merck. Aniline was distilled under reduced pressure and other reagents were used as received without further treatment. All solutions were prepared with deionized water.

Morphology and particle sizes of composites were noticed using by transmission electron microscopy (TEM, PHILIPS, CM10-HT, 100 kV) and energy-dispersive X-ray spectrometry (EDX) was performed by an EDX detector on a HITACHI, 4160 scanning electronic microscope (SEM) with a voltage of 15 kV. X-ray diffraction patterns were taken on a SIEMENS (D5000) X-ray diffractometer with CuKα radiation, at a 10°/min scanning speed from 2° to 90° (in 2θ). Ultraviolet visible (UV–vis) absorption spectra were taken using a SHIMADZU (UV-1601PC) spectrophotometer. Fourier transform infrared spectroscopy (FTIR) was performed on a Bruker model Tensor Fourier transform spectrometer in the range of 400–4000 cm^{-1} using KBr pressed disks. Electrochemical experiments were conducted using Autolab instrument (PGSTATE12) in a three-electrode system. All electrochemical experiments were performed in a cell containing 20 mL of phosphate buffer solution (PBS, 0.1*M*) at room temperature and using platinum wire as the auxiliary, a saturated calomel electrode (SCE) as the reference, and the AgCl/PANI/PVA modified glassy carbon electrode (GCE) as the working electrode. All experimental solutions were deaerated by bubbling highly pure nitrogen for 10 min, and a nitrogen atmosphere was kept over the solutions during electrochemical measurements.

Synthesis of AgCl/PANI Nanocomposite in PVA Matrix

AgCl/PANI/PVA nanocomposite was synthesized through a two-stage process. First, the positively charged Ag NPs were prepared by borohydride reduction of $AgNO_3$ salt solution as detailed by Sun *et al.*[22] with some modification. Briefly, 2 mL 4-ATP ethanol solution (1 m*M*) was poured to 20 mL silver nitrate solution (0.5 m*M*) under vigorous stirring. After the dissolution of 4-ATP, 0.4 mL of freshly prepared aqueous sodium borohydrid solution (10 m*M*) was injected dropwise into the solution under vigorous stirring. Then, the silver clear black brown colloids were centrifuged twice at 8000 rpm for 20 min and the obtained precipitates were removed. Then, the AgCl/PANI/PVA

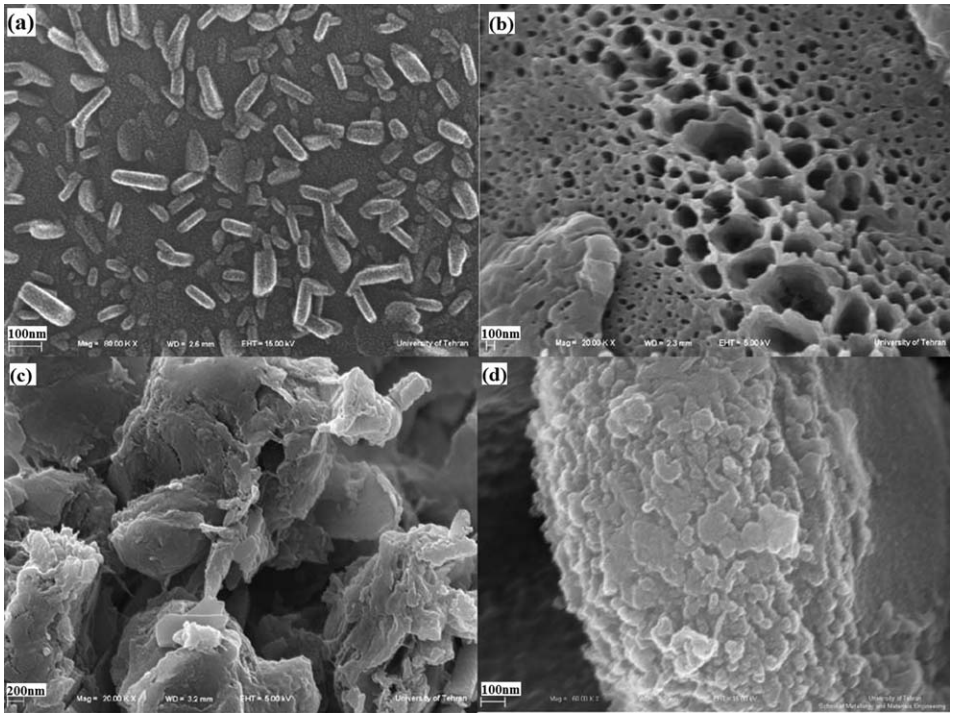

Figure 4. SEM images of (a) AgCl/PANI/PVA (composite 1) (b) filtrate of composites 1 (c) Ag oxides/CSA/PANI/PVA (composite 3) (d) Ag/PANI/PVA (composite 4).

nanocomposite (composite 1) was prepared by chemical polymerization of aniline in the following approach:

PVA polymer powder (1 g) was fully dissolved in 100 mL of deionized water in a silicone oil bath at 90°C. The obtained 1 wt % PVA solution was allowed to cool to room temperature and then silver NPs colloid with pH 3.5 were added to the PVA solution and stirred at room temperature. The resulted mixture had pH 4.5. After the adjusting of the pH 3 with concentrated HCl, aniline (0.35 g) and APS (0.78 g) as oxidant were dropped into the mixture and was maintained under magnetic stirring for 4 h at room temperature. The molar ratio of aniline to APS ([An] : [APS]) was 1 : 1. The product was filtered and thoroughly washed with deionized water and methanol to remove nonreacted monomer, oligomer, and excess of oxidant. Obtained composite was dried in vacuum at 40°C for 24 h (composite 1), while the filtrate was kept for freeze dry in order to remove water, finally yielding a green compound after freeze drying. The reaction was carried out under other acidic mediums similar to composite 1, with adjusting pH = 4 with HCl (Ag/AgCl/PANI/PVA, composite 2), pH = 3 with CSA (Ag oxides/CSA/PANI/PVA, composite 3) and in the absence of acid medium (Ag/PANI/PVA, composite 4). Obtained composites were purified and dried similar to composite 1.

RESULTS AND DISCUSSION

AgCl/PANI/PVA nanocomposite was successfully synthesized via chemical polymerization of aniline in the presence of positively-charged Ag NPs, HCl, and PVA. PVA is a biocompatible polymer and resulted AgCl/PANI nanocomposite in the presence of it could be having potential in biological activities. First, AgNPs were synthesized by borohydride reduction of $AgNO_3$ in the presence of 4-ATP as stabilizer, and then the polymerization of aniline was carried out in the presence of HCl, APs, and PVA. Positively charged Ag NPs could be reacted with chloride ions to obtain AgCl NPs. Also, polymerization of aniline was carried out in the three different acidic media.

Figure 1 shows the UV–vis spectra of Ag NPs colloid and synthesized composites 1, 3, 4, and the filtrate of composite 1. As shown in Figure 1(A) (a), colloidal AgNPs exhibit absorption band or broad region of absorption at around 425 nm which arise from excitation of plasmon resonances or interband transitions.[16,23] Surface plasmon absorption position of metal NPs is mainly sensitive to a number of factors, such as particle size, shape, and the nature of the surrounding media.[24] Characteristic peak of composites was appeared at around of 390 nm which is attributed to π–π^* transition [Figure 1(A), (b–d)].[25] Also, characteristic peaks of filtrate of composite 1 were appeared at 360, 410, and 750 nm which are attributed to π–π^*, polaron–π^*, and localized polaron–π transitions of doped PANI, respectively [Figure 1(B)].[26] The results indicate that the filtrate of AgCl/PVA/PANI nanocomposite can essentially be considered as PANI/PVA. From UV–vis spectra of composites, it is observed that characteristic peaks for the polaron–π^* and π–polaron transitions of polyaniline are absent [Figure 1(b–d)][27] which this could be related to the strong interaction among metal NPs, PVA, and PANI.

The composition and the structure of the products were characterized with EDX and XRD. Figure 2 shows the XRD pattern of composites 1, 2, 3, 4 and filtrate of nanocomposite 1. In XRD pattern of the composite 2, diffraction peaks at $2\theta = 6.6$, 19, 23.4° and 25.8° are associated with organization, periodicities parallel and perpendicular of the PANI chains, respectively[28,29] [Figure

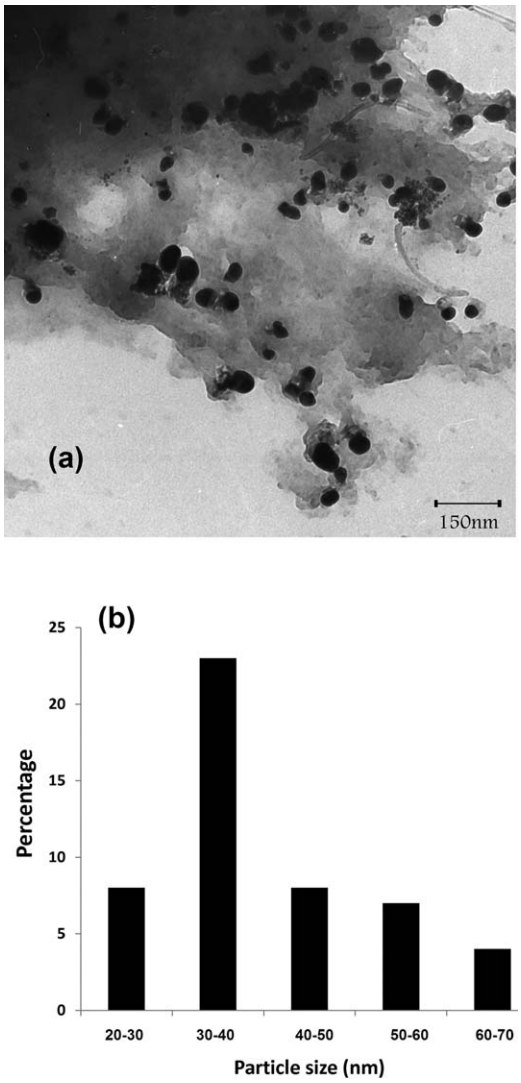

Figure 5. TEM images of (a) AgCl/PANI/PVA (composite 1), (b) size distribution of AgCl NPs in AgCl/PANI/PVA nanocomposite.

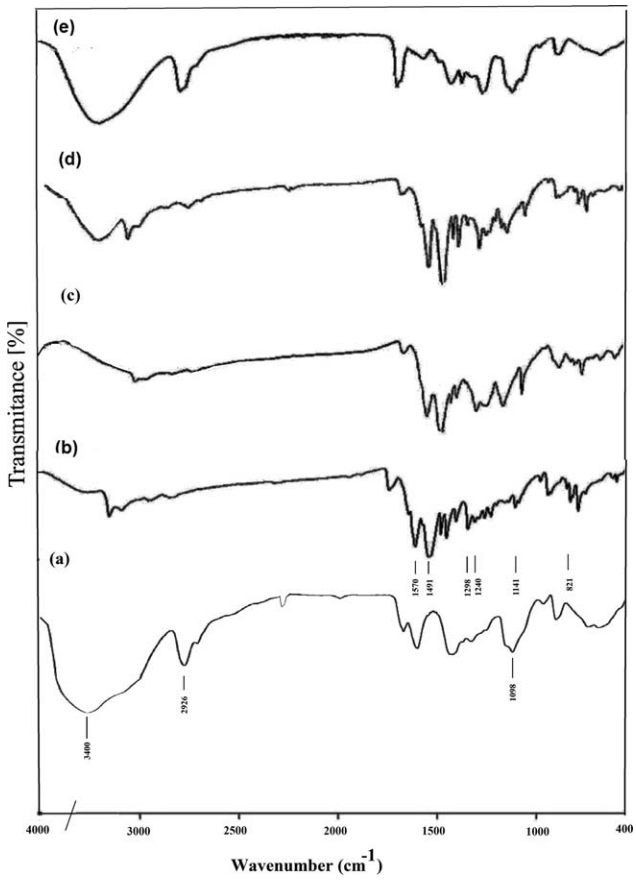

Figure 6. FT-IR spectrum of (a) pure PVA (b) AgCl/PANI/PVA (composite 1) (c) Ag Oxides/CSA/PANI/PVA (composite 3) (d) Ag/PANI/PVA (composite 4) (e) filtrate of composite 1.

2(A) (a)]. The appeared peaks at $2\theta = 27.9$, 32.4, 46.2, 54.8, 57.5, 67.7, 74.6, and 76.7 are related to scattering forms of (111), (200), (220), (311), (222), (400), (331), and (420) of AgCl NPs, respectively and the other peaks at $2\theta = 38$ and 44.5 are due to Ag NPs [Figure 2(a)].[30,31] These results indicate that most of positively charged AgNPs reacted with chloride ions to form AgCl nanoparticles. When the pH of reaction mixture was decreased until pH = 3, the peaks of Ag NPs was disappeared and only the peaks of AgCl NPs were shown [Figure 2(A) (b)]. In the XRD of the filtrate of composite 1 appears a peak at $2\theta = 19.77$ which is related to overlapped peaks of PANI and PVA [Figure 2(A) (c)]. The results show that precipitate of composite 1 is as AgCl/PANI/PVA and the filtrate of it is as PANI/PVA. With changing of acidic medium to CSA [Figure 2(A) (d)], the structure of composite changed and peaks of AgCl NPs were disappeared. Figure 2(A) (d) implies a peak at $2\theta = 19$ related to overlapped peaks of PVA and PANI and the new peaks at $2\theta = 26$, 32, 39 related to Ag oxides (AgO and Ag_2O) structures.[32] In the absence of acid medium (pH = 5.5), the peak centered at $2\theta = 19$ related to overlapped peaks of PANI and PVA[21] and the peaks of Ag NPs were appeared at $2\theta = 38$ and 44.5 with low intensity [Figure 2(B)]. XRD results show that in different acidic solutions, positively-charged AgNPs can be appeared as Ag, AgCl, AgO, and Ag_2O NPs and the pH of reaction has most important effect on the structure of obtained composites.

The elemental compositions of the composites 1, 3, 4 and the filtrate of composite 1 are shown by EDX analysis in Figure 3. Figure 3(a) depicts the EDX spectrum of the composite 1 and it is deduced that the weight % of Ag is 2.85 and in view of the significant amount of Ag present, we designate the precipitate as AgCl/PANI/PVA composite, while the EDX spectrum depicted in Figure 3(b) indicates no wt % of Ag so the filtrate can essentially be considered as PANI/PVA. Also, the EDX spectrum of the composites 3 and 4 shows the presence of Ag with weight % 1.04 and 1.34, respectively. EDX analysis shows that the weight % of Ag in AgCl/PANI/PVA composite is high compared to other composites which this could be related to chloride ions.

The SEM pictures of the composites 1, 3, 4, and filtrate of composite 1 are shown in Figure 4(a–c). From the SEM image, it is observed that composite 1 display a capsulated morphology with average particle size ranges between 50 and 160 nm with the maximum close to 100 nm in polymer matrix. The possible

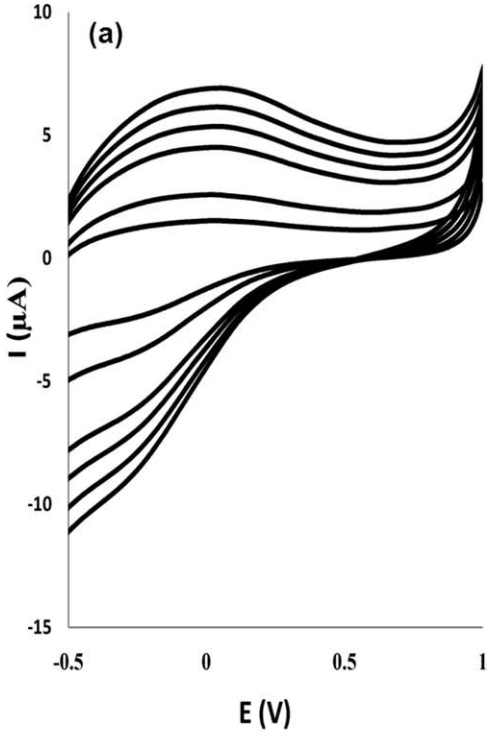

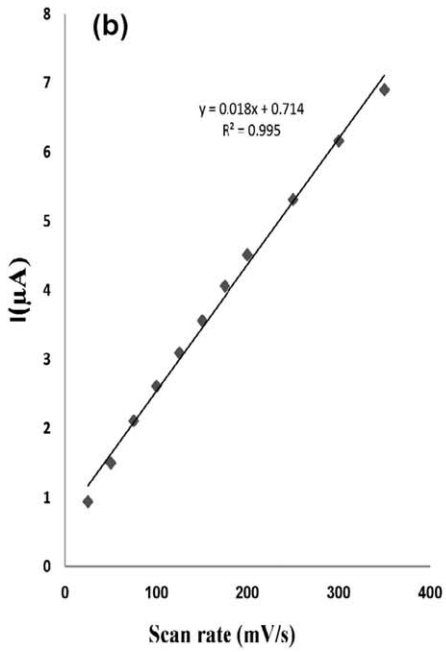

Figure 7. (a) Cyclic voltammograms of AgCl/PANI/PVA/GC in the potential scan rates in the range of 25–350 mV s^{-1}. (b) Dependence of the anodic currents of AgCl/PANI/PVA/GC on scan rates in PBS (pH 7.4).

mechanism for the formation of AgCl/PANI/PVA nanocomposite can be said the following method:

In HCl medium, chloride (Cl^-) ions were adsorbed on the surface of AgNPs and then AgCl NPs acted as first nucleation of composite and PANI were wrapped around of AgNPs to obtain capsulated AgCl/PANI nanocomposite in PVA matrix. SEM

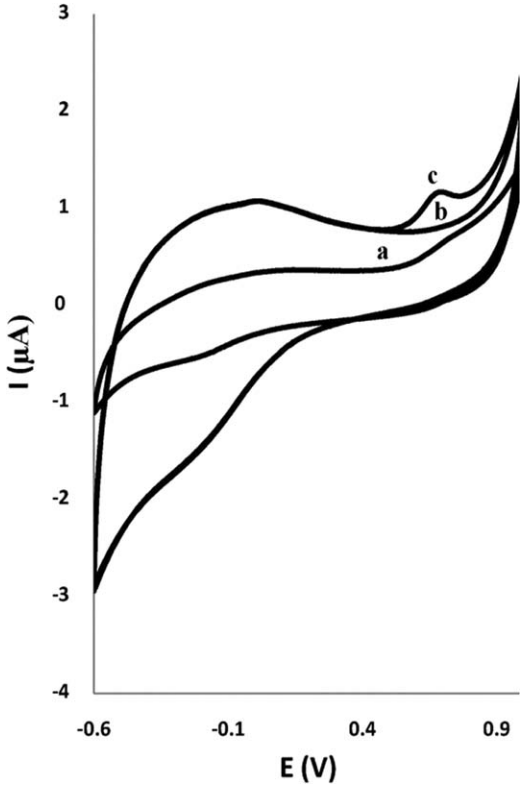

Figure 8. Cyclic voltammograms of the (a) bare GCE in the presence of 100 μ*M* of DA (b) AgCl/PANI/PVA/GC in the absence (c), and presence of 100 μ*M* of DA, scan rate is 50 mVs^{-1}.

image of freeze dried filtrate of composite 1 [Figure 4(b)] shows porous structure which could be originated from interactions between PANI and PVA. With changing of acidic media to CSA [Figure 4(c)] or elimination of acidic media [Figure 4(d)], fused and aggregated structures of composites were appeared. SEM images confirm the important effect of acidic medium on the morphology of resulted composites.

Figure 5 shows the TEM image and histogram of particle size distribution of AgCl NPs inside of resulted nanocomposite. As shown in TEM image [Figure 5(a)], AgCl NPs (black spots) are well dispersed in polymer matrix due to strong affinity of AgCl for nitrogen and oxygen. The average particle size of AgCl ranges between 20 and 70 nm with the maximum close to 40 nm. The surrounding PANI isn't distinguished because of high interaction between PANI and PVA.

Figure 6 shows the FT-IR spectra of composites 1, 3, 4, filtrate of composite 1 and a pure PVA sample as a reference in 400 to 4000 cm^{-1} region. The pure PVA sample [Figure 6(a)] shows the typical C—H alkyl stretching band at 2926 cm^{-1} and the hydrogen bonded hydroxyl band at 3400 cm^{-1}. The peak at 1096 cm^{-1} is related to the C—O stretching vibration of the secondary alcohol (CH—OH) of PVA.[21] The characteristic bands of PVA were appeared in the FT-IR spectra of composites and this represents the presence of PVA [Figure 6(b–e)]. For the composites 1, 3, and 4, it was noticed there was a shift and a decrease in the peak intensity at 3400 cm^{-1} which could be related to the presence of PANI [Figure 6(b–d)]. For the

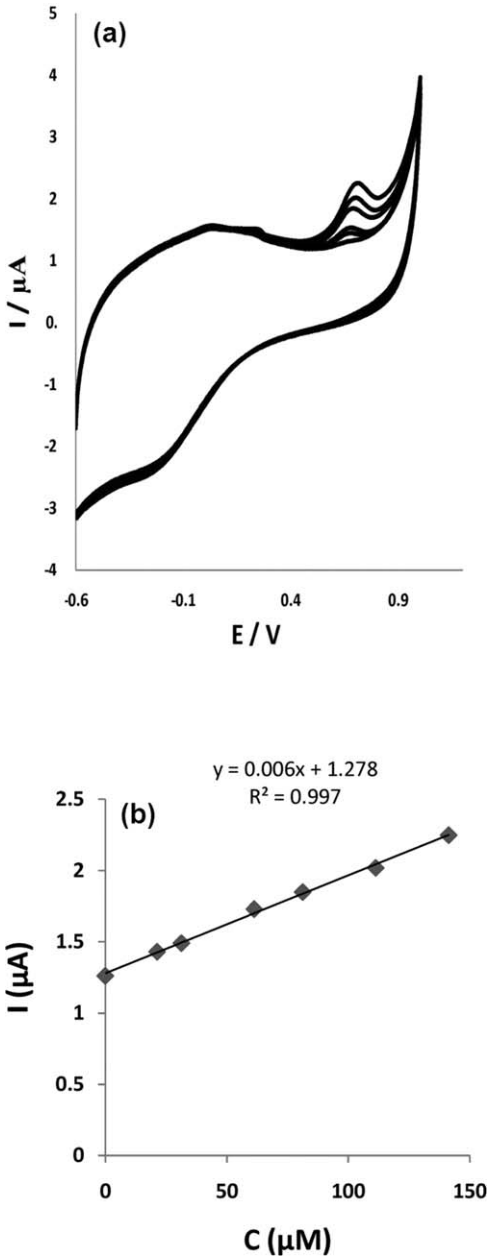

Figure 9. (a) Cyclic voltammograms of AgCl/PANI/PVA/GC in the presence of different DA concentrations. The potential scan rate is 50 mV/s. (b) Dependency of the anodic current electro-oxidation on DA concentration in the range of 21.3–141.3 µ*M*.

composites, there were also new peaks assigned to PANI.[25] The characteristic bands at 1570 and 1491 cm^{-1} correspond to C═C stretching of the quinoid and benzoid rings, respectively.[25] The C—N and C═N stretching modes were appeared at 1298 and 1240 cm^{-1}, respectively. The absorption peak at 1141 cm^{-1} is assigned to the in-plane bending of C-H, and the peak at 821 cm^{-1} is attributable to C—H bending vibration out of the plane of the *para*-disubstituted benzene rings.[33] In the FT-IR spectra of filtrate of composite 1 were appeared characteristic peaks of PANI with low intensity which could be related to interactions between PVA and PANI [Figure 6(e)].

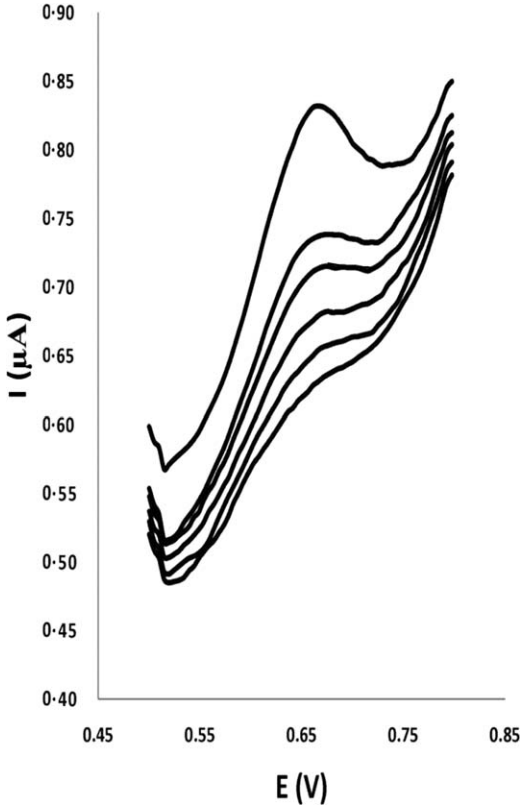

Figure 10. Differential pulse voltammograms of AgCl/PANI/PVA/GC in different concentrations of DA.

Cyclic voltammetric experiments were performed to test the electroactivity of the AgCl/PANI/PVA nanocomposite. The bare GCE was previously tested in different pH phosphate buffer solutions (PBS) before the AgCl/PANI/PVA nanocomposite was drop-coated onto it. It presents no redox process in the potential range studied. To assure diffusion of the solution into the interlayer space and to permit better ionic exchange, the working electrode coated with the nanocomposite is immersed in the electrolyte solution for 20 min prior to the measurement. Figure 7 shows the effect of the potential scan rate (v) on the peak current for the AgCl/PANI/PVA modified electrode in the range of 25–350 mV s^{-1} in 0.1*M* PBS (pH = 7.4). With the increase in scan rate, the anodic and cathodic peak currents increase. The anodic peak currents for nanocomposite increase linearly with the scan rate, indicating surface controlled process.[34] A broad peak is observed for the sample with the redox potential at around −57 mV which is related to the overlap of two redox processes of leucoemeraldine to emeraldine salt and emeraldine salt to the pernigraniline state.[35]

The electrocatalytic activity of AgCl/PANI/PVA nanocomposites was examined in the anodic oxidation of DA because it is an important neurotransmitter in mammalian brain system and the loss of DA-containing neurons may cause serious diseases such as Parkinson.

The electrochemical behaviors of the bare and modified electrodes were investigated by cyclic voltammogram (CV) in 0.1*M* PBS (pH 7.4) containing 100 µ*M* DA. As shown in Figure 8(a),

Table I. Analytical Parameters for Detection of DA at Previously Reported Methods

Type of analyte	Sensor	pH	Method	Linear range	LOD	Refs.
DA	Boron-doped CNT/GCE	7	DPV	20–7500 μM	1.4 μM	35
	MCNT-poly(DBA)/GCE	7.4	Amperometry	10–70 nM	0.1 nM	36
	EDTA-GS/Nafion/GCE	7.2	CV	0.2–25 nM	0.1 nM	37
	PTCA-GS/MCNT/IL/GCE	5	Amperometry	30–3,800,000 nM	1.2 nM	38
	Ag/PANI/GC	3	DPV	18.5–72.2 μM	2 μM	39
	AgCl/PANI/PVA	7.4	DPV	80–250 μM	17 3 μM	This work

GCE: glassycarbonelectrode; CNTs: carbonnanotubes; MCNTs: multiwallcarbonnanotubes; IL: ionic liquids;GS: graphenesheets; poly(DBA): poly(3,5-dihydroxybenzoicacid); PTCA-GS: 3,4,9,10-perylenetetracarboxylicacidfunctionalized graphene sheets.

a weak anodic current appeared on the bare GCE with an anodic peak (Epa) at 670 mV, which indicated the direct electron transfer of DA on bare GCE was very slow. In contrast, the anodic current significantly increases for GCE/AgCl/PANI/PVA electrode in the presence of DA [Figure 8(c)]and oxidation peak shifted to negative potential (630 mV) and as can be seen in absence of DA, GCE/AgCl/PANI/PVA shows no peak at 670 mV. The higher redox current and more negative oxidation potential suggested that GCE/AgCl/PANI/PVA have good electrocatalytic ability to the electrochemical reaction of DA.

Increasing of oxidation peak currents with the gradual addition of DA confirms the catalytic property of the GCE/AgCl/PANI/PVA in the oxidation of DA (Figure 9). GCE/AgCl/PANI/PVA exhibits a linear response to DA in the concentration range of 21–141 μM with a correlation coefficient of 0.997 (Figure 9, inset).

The differential pulse voltammetry (DPV) was used for the determination of DA under the optimum conditions. Figure 10 shows differential pulse voltammograms obtained at GCE/AgCl/PANI/PVA in various concentrations of DA. The peak currents were proportional to DA concentration in the range of 80–250 μM with a detection limit of 17.2 μM ($S/N = 3$). A comparison of the AgCl/PANI/PVA modified electrode with other reported modified electrodes for DA detection is listed in Table I.[16,36–39] It can be seen that the proposed method was fairly sensitive and has an LOD of 17.3 μM in a neutral solution whereas other electrode provided lower LODs. But AgCl/PANI/PVA provided wide linear range for detection of these molecules. It could be seen that the AgCl/PANI/PVA offered reasonable linear ranges for DA detection in a neutral solution, while Ag/PANI/GC showed electrocatalytic activity in acidic condition. DPV and CV experiments showed that the detection DA by GCE/AgCl/PANI/PVA is appropriate.

Additional experiments were done to test the stability of AgCl/PANI/PVA nanocomposite. It was found that no obvious changes for the catalytic peak current were found for GCE/AgCl/PANI/PVA in air for 10 days which returns the good stability of the nanocomposite. In addition, no significant decrease can be seen after replacing the electrolyte having been used for 100 repetitive cycles with fresh solution. These results indicated that GCE/AgCl/PANI/PVA is a proper platform for the determination of DA.

CONCLUSION

Capsule like AgCl/PANI nanocomposite inside PVA matrix was successfully synthesized through chemical polymerization of aniline in the presence of colloidal Ag NPs and HCl medium (pH = 3). The resulted Ag NPs from borohydride reduction of $AgNO_3$ in the presence of 4-ATP could provide more active sites for the nucleation of polyaniline and also could with chloride ions were converted to AgCl NPs to obtained AgCl/PANI/PVA. The preparation of composite was also carried out in the absence of acid and presence of camphorsulfonic acid as the acidic medium. XRD analysis and SEM images showed with changing of acidic medium, agglomerated particles with different structures were appeared in comparison with the product obtained in HCl medium. Furthermore, AgCl/PANI/PVA nanocomposite was immobilized on the GCE and the electroactivity of nanocomposite was investigated through CV and DPV. The GCE/AgCl/PANI/PVA showed electrocatalytic activity for the oxidation of DA in neutral medium. The nanocomposite may have a great potential in designing sensitive biosensors, biological separators, and enzyme immobilization.

ACKNOWLEDGMENTS

The authors of this research were financially supported by the Payame Noor University of Iran.

REFERENCES

1. Tian, S.; Liu, J.; Zhu, T.; Knoll, W. *Chem. Mater.* **2004**, *16*, 4103.
2. Griesser, T.; Radl, S. V.; Koepplmayr, T.; Wolfberger, A.; Edler, M.; Pavitschitz, A.; Kratzer, M.; Teichert, C.; Rath, T.; Trimmel, G. *J. Mater. Chem.* **2012**, *22*, 2922.
3. Gao, Y.; Shan, D.; Cao, F.; Gong, J.; Li, X.; Ma, H. Y.; Su, Z. M.; Qu, L. Y. *J. Phys. Chem. C* **2009**, *113*, 15175.
4. Zhou, W.; Yu, Y.; Chen, H.; Di Salvo, F. J.; Abruña, H. D. *J. Am. Chem. Soc.* **2013**, *135*, 16736.
5. Xian, Y.; Hu, Y.; Liu, F.; Xian, Y.; Wang, H.; Jin, L. *Biosens. Bioelectron.* **2006**, *21*, 1996.
6. Xue, W.; Qiu, H.; Fang, K.; Qiu, H.; Li, J.; Mao, W. *Synth. Met.* **2006**,*156*, 833.
7. Ward, R. E.; Meyer, T. Y. *Macromolecules* **2003**, *36*, 4368.

8. Huang, J.; Moore, J. A.; Acquaye, J. H.; Kaner, R. B. *Macromolecules* **2005**, *38*, 317.
9. Peng, X.; Manna, L.; Yang, W.; Wickham, J.; Scher, E.; Kadavanich, A.; Alivisatos, A. P. *Nature* **2000**, *404*, 59.
10. Tseng, R. J.; Huang, J.; Ouyang, J.; Kaner, R. B.; Yang, Y. *Nano Lett.* **2005**, *5*, 1077.
11. Potiyaraj, P.; Kumlangdudsana, P.; Dubas, S. T. *Mater. Lett.* **2007**, *61*, 2464.
12. Tiwari, J.; Rao, C. R. *Solid State Ionics* **2008**, *179*, 299.
13. Hu, W.; Chen, S.; Li, X.; Shi, S.; Shen, W.; Zhang, X.; Wang, H. *Mater. Sci. Eng. C* **2009**, *29*, 1216.
14. Choi, M.; Shin, K. H.; Jang, J. *J. Colloid Interface Sci.* **2010**, *341*, 83.
15. An, C.; Wang, R.; Wang, S.; Zhang, X. *J. Mater. Chem.* **2011**, *21*, 11532.
16. Massoumi, B.; Fathalipour, S.; Massoudi, A.; Hassanzadeh, M.; Entezami, A. A. *J. Appl. Polym. Sci.* **2013**, *130*, 2780.
17. Choudhury, A.; Kar, P.; Mukherjee, M.; Adhikari, B. *Sens. Lett.* **2009**, *7*, 592.
18. Zhang, Q.; Liu, F.; Li, L.; Pan, G.; Shang, S. *J. Nanoparticle Res.* **2011**, *13*, 415.
19. Feng, X.; Liu, Y.; Lu, C.; Hou, W.; Zhu, J. J. *Nanotechnology* **2006**, *17*, 3578.
20. Zhou, S.; Xie, M.; Yuan, X.; Zeng, F.; Zou, W.; Yuan, D. *Am. J. Anal. Chem.* **2012**, *3*, 385.
21. Bhadra, J.; Sarkar, D. B. *Mater. Sci.* **2010**, *33*, 519.
22. Sun, L.; Wei, G.; Song, Y.; Liu, Z.; Wang, L.; Li, Z. *Appl. Surf. Sci.* **2006**, *252*, 4969.
23. Zhang, J.; Li, X.; Liu, K.; Cui, Z.; Zhang, G.; Zhao, B.; Yang, B. *J. Colloid Interface Sci.* **2002**, *255*, 115.
24. Tao, A. R.; Habas, S.; Yang, P. *Small* **2008**, *4*, 310.
25. Xia, H.; Wang, Q. *Chem. Mater.* **2002**, *14*, 2158.
26. Reddy, K. R.; Lee, K. P.; Gopalan, A. I.; Kim, M. S.; Showkat, A. M.; Nho, Y. C. *J. Polym. Sci. A: Polym Chem.* **2006**, *44*, 3355.
27. Yu, Q.; Shi, M.; Cheng, Y.; Wang, M.; Chen, H. Z. *Nanotechnology* **2008**, *19*, 265702.
28. Pouget, J.; Jozefowicz, M.; Epstein, A.; Tang, X.; MacDiarmid, A. *Macromolecules* **1991**, *24*, 779.
29. Tung, N. T.; Lee, H.; Song, Y.; Nghia, N. D.; Sohn, D. *Synth. Met.* **2010**, *160*, 1303.
30. Kim, S.; Chung, H.; Kwon, J. H.; Yoon, H. G.; Kim, W. *Bull. Korean Chem. Soc.* **2010**, *31*, 2918.
31. Jin, R.; Cao, Y.; Mirkin, C. A.; Kelly, K.; Schatz, G. C.; Zheng, J. *Science* **2001**, *294*, 1901.
32. Liu, J.; Sonshine, D. A.; Shervani, S. R.; Hurt, H. *ACS Nano* **2010**, *4*, 6903.
33. Paulraj, P.; Janaki, N.; Sandhya, S.; Pandian, K. *Colloid Surf. A* **2011**, *377*, 28.
34. Basavaraja, C.; Veeranagouda, Y.; Kim, N. R.; Jo, E. A.; Lee, K.; Huh, D. S. *Bull. Korean Chem. Soc.* **2009**, *30*, 1097.
35. Tang, Y.; Pan, K.; Wang, X.; Liu, C.; Luo, S. *J. Electroanal. Chem.* **2010**, *639*, 123.
36. Deng, C.; Chen, J.; Wang, M.; Xiao, C.; Nie, Z.; Yao, S. *Biosens. Bioelectron.* **2009**, *24*, 2091.
37. Zhu, Z.; Qu, L.; Guo, Y.; Zeng, Y.; Sun, W.; Huang, X. *Sens. Actuat. B: Chem.* **2011**, *151*, 146.
38. Wu, L.; Feng, L.; Ren, J.; Qu, X. *Biosens. Bioelectron.* **2012**, *34*, 57.
39. Zhu, H.; Du, M.; Zhang, M.; Wang, P.; Bao, S.; Wang, L.; Fu, Y.; Yao, J. *Biosens. Bioelectron.* **2013**, *49*, 210.